Mechanical Properties and the Two-Phase Structure Inside the Heterophase Domains of Blends from HDPE and SBS Star Block Copolymers

N. STRIBECK,[1] C. REIMERS,[1] P. GHIOCA,[2] E. BUZDUGAN[2]

[1] Institut für Technische und Makromolekulare Chemie, Universität Hamburg, 20146 Hamburg, Germany

[2] Chemical Research Institute ICECHIM, 77208 Bucharest, Romania

Received 27 February 1997; revised 26 November 1997; accepted 2 December 1997

ABSTRACT: Blends from polyethylene (PE) and polystyrene-*b*-polybutadiene-*b*-polystyrene star block copolymers (SBS) (thermoplastic elastomers) are studied with polyolefine recycling in view. Each component, dispersed in a heterogeneous blend, exhibits a two-phase morphology. This structure is investigated by small angle X-ray scattering (SAXS) and compared to mechanical properties as a function of SBS grade and content. Increasing the SBS content one observes a vanishing PE-related long period reflection, while an SBS-related peak emerges. Best mechanical properties are obtained at concentrations, where the width of the observed long period reflection is broadest. For a quantitative analysis of the SAXS, the interface distribution function (IDF) analysis is employed. Data are fitted with a function modeling arrangement as well as disorder of domains inside the two different kinds of dispersed grains. The analysis yields that the observed broadening of the long spacing peak is caused only by an increased fluctuation of the thicknesses of amorphous layers in the PE stacks. This fluctuation again decreases for SBS concentrations beyond 15 wt %. The effect is strongest for blends containing the SBS grade with the lowest molecular weight and is discussed in terms of its compatibilization effect. © 1998 John Wiley & Sons, Inc. J Polym Sci B: Polym Phys 36: 1423–1432, 1998

Keywords: recycling; polyolefine modification; mechanical properties; SAXS; disorder; compatibilizer; blend; block copolymers; polyethylene

INTRODUCTION

Blending of polymers is a common technology, frequently applied in order to develop high performance materials. Searching for synergistic effects, one expects to find a product with superior mechanical properties, which is made from inexpensive polymer material and small amounts of compatibilizers. One of the cheapest polymer materials is collected postconsumer plastics. Here the question is how to raise performance to a sufficient level. In this field of dispersed heterogeneous blends the class of polystyrene-*b*-polybutadiene-*b*-polystyrene (SBS) block copolymers and their hydrogenated and functionalized derivatives plays an important role. The reason is that such additives act both as impact modifiers and as compatibilizers.

Recent articles report improvements of mechanical properties by addition of SBS not only to commingled plastic waste,[1] but also to blends of polyethylene (PE) and polystyrene (PS),[2] to blends of polypropylene (PP) and PS,[3] and even to homopolymer PP and PE.[4,5,6] These plastomers are frequently regarded as model substances for plastics waste. Most of the articles[1,2,3,5] link me-

Correspondence to: N. Stribeck

Journal of Polymer Science: Part B: Polymer Physics, Vol. 36, 1423–1432 (1998)
 CCC 0887-6266/98/091423-10

Table I. Characterization of Three SBS Star Block Copolymers to be Blended with HDPE. All Grades Have Four Arms, Except an Amount of 9% Uncoupled Diblock Copolymer. The PB Contains 10% of (1,2)-PB. Naming is Derived from Molecular Weight and PS Content. S1429 is the Commercial Product Finaprene® 416

Block Copolymer	M_W [g/mole]	Wt Fraction PS
S1429	135,000	0.29
S1846	178,000	0.46
S3530	350,000	0.30

chanical properties to structural findings obtained by electron microscopy, but a small-angle X-ray scattering (SAXS) study is unknown to us. While electron microscopy can be used even to study shape and arrangement of "heterophase domains" on a micrometer scale, SAXS generally exhibits only the "fine structure" inside these grains (with periods in the order of magnitude of 10 nm). Inside the PE grains, this fine structure arises from the contrast between crystalline and amorphous domains. Inside the SBS grains, one studies PS domains in a polybutadiene (PB) matrix.

A commercial high density PE (HDPE) with low molecular weight is chosen as a model for collected postconsumer PE, and is blended with various commercial grades of SBS. In a preceding article[7] we have already reported on the observation of density undulations in these samples. The undulations are clear but of low amplitude, have a period of 5 nm and range over a distance of 40 nm. The effect is reproducible, can be observed in the pure PE, is strongest in blends which contain about 10 wt % of SBS, and is not found in blends with more than 20 wt % of SBS. Now we present mechanical data and correlate these with the structural findings of the SAXS data analysis.

MATERIAL

The main component of the blends is a high density polyethylene, Argetena J, manufactured by Arpechim S. A. Corp., Pitesti, Romania. Its weight average molecular weight is $\bar{M}_w$ = 42,000 g/mole. From the measured density ρ = 0.965 g/cm^3 one computes a volume crystallinity Φ_c = 0.76.

Three different SBS grades are blended with this HDPE. They are characterized in Table I. All grades are star block copolymers with four arms. The elastomer content of the blends ranges from zero to 30 wt % in steps of 5 wt %. Reproducibility of the process has been verified and documented elsewhere.[7,8]

Blending takes 9 min and is carried out in air. Three hundred g PE is dumped on a mill (150°C) made of two rollers rotating with different speed (factor 1.2). After 3 min the PE is molten and SBS is added. In order to improve intermixing, several times during the blending process the film has been cut, stripped off, folded and fed again. Then the sheet is cooled to ambient temperature. After a resting period of 1 day the material is pressed (165°C, 15 min, 170 bar) into plates of uniform thickness (1–2 mm).

METHODS

SAXS is measured using Ni-filtered CuK_α-radiation and a Kratky camera. A moving slit device serves for calibration to absolute intensity units and for the determination of sample absorption. Recorded curves cover the interval from s = 0.01 nm^{-1} to s = 0.6 nm^{-1}. $s = (2/\lambda)\sin\theta$ is the magnitude of the scattering vector with λ being the wavelength of radiation and θ being half of the scattering angle.

Straining is carried out on a Zwick 1454 stretching machine at a strain rate of 50 mm/min using standard test bodies (DIN 53455, No. 4) punched from the polymer plates. Impact resistance is measured according to the Izod procedure.

The density of every sample has been measured in a density gradient prepared from formic acid and 1-propanol. The gradient has been calibrated with glass floats.

TEM micrographs have been obtained from sections of ca. 100 nm thickness, stained with O_sO_4.

DATA EVALUATION

Kratky camera data are quantitatively evaluated using the method of interface distribution function (IDF) analysis[9] fitting a generalized model for stacking statistics.[10]

The Nonideal Multiphase System

Subtraction of the instrumental background (after multiplication by the absorption factor of the sample) is the first step of data evaluation.

After that the scattering curve is calibrated in absolute intensity units.

If SAXS data from multiphase systems are analyzed, the nonideal nature of the domains leading to systematic deviations[11] from Porod's law must be considered. In the asymptotic limit ($s \to \infty$) Porod's law predicts a decrease of the ideal slit-smeared SAXS intensity, $\tilde{I}(s)/V$, with $\tilde{A}_P/s^3$. Polymers, in general, exhibit a considerable density fluctuation background, $\tilde{I}_{Fl}/V$, arising from fluctuations of the electron density inside a single phase. Moreover, ideal multiphase systems are supposed to exhibit an instant jump of density when crossing the phase boundary (interface). Thus it appears reasonable for real samples to consider a smooth transition zone characterized by introduction of a width parameter σ_t. Since both mentioned effects alter the power law of the SAXS tail in a different manner, the corresponding parameters can both be determined from the tail of the curve, if only the curve has been measured with sufficient accuracy over a wide angular range. Because the studied samples show an extraordinary long and well-defined region where Porod's law appears to be valid, we can determine the parameters directly by computing a *slit-smeared interference function*

$$\tilde{G}_{id}(s) = \frac{(\tilde{I}(s)/V - \tilde{I}_{Fl}/V)s^3}{(1 - 8\pi^2\sigma_t^2 s^2)\mathrm{erfc}(2\pi\sigma_t s) + 4\sqrt{\pi\sigma_t s}\,\exp[-4\pi^2\sigma_t^2 s^2]} - \tilde{A}_P \quad (1)$$

of the ideal multiphase system and varying both values, until $\tilde{G}_{id}(s)$ vanishes in the Porod region. While a variation of $\tilde{I}_{Fl}/V$ bends the curve, a variation of $d_t = 3\sigma_t$ tilts it. In eq. (1) the numerator holds the fluctuation background subtraction and the multiplication by Porod's power law. Its denominator is only a function of the transition zone at the phase boundary (interface). Finally, $\tilde{A}_P$, is a constant which governs the slit-smeared Porod's law of any ideal multiphase sample. In the long Porod region of this $\tilde{G}_{id}(s)$ function a peak of triangular shape is observed, which can be interpreted in terms of faint electron density undulations, as mentioned in the section "Introduction." After removal of this peak from $\tilde{G}_{id}(s)$ one computes a scattering intensity

$$\tilde{I}_{id}(s)/V = \frac{1}{s^3}(\tilde{G}_{id}(s) + \tilde{A}_P) \quad (2)$$

which one would have measured from a sample with ideal multiphase structure. Thus $\tilde{I}_{id}(s)/V$ describes the scattering of a sample containing domains with uniform density inside and an ideal density step at each interface. Although we are now considering such an ideal multiphase system, this does not imply that the domains must be convex bodies. In particular, the domain surface may be roughened by peaks and valleys (or fingers and holes) emerged or imprinted with respect to an imaginated smooth surface. As long as one does not assume self-similarity in this model (e.g., warts on the fingers and hair on the warts), Ruland[12] and Semenov[13] have shown that such interfacial roughness does not cause the scattering curve to fall away less sharply than Porod's law, as, on the other hand, it is predicted by the scattering of a surface fractal. Instead, one observes an increased asymptote $\tilde{A}_P$ or, with respect to the chord distribution of the domain-matrix-system, many chords of extremely short length. *Chords* are straight lines, connecting two surface points (of the domains).

The IDF Analysis

If one does not intend to interpret the results of a SAXS experiment directly in reciprocal space, one can obtain the correlation function[14,15] in physical space by a Fourier transform of the scattering curve and interpret it. For a two-phase system from stacked layers one suitably computes the one-dimensional correlation function,[16] from which values of the average layer thicknesses of both phases can be extracted by application of a simple graphical evaluation method.

Even if the correlation function is defined in physical space and thus closer to our notion than the scattering curve, its interpretation is frequently limited to the determination of "crystallinity" and long period in the lamellar stack. However, since the work of Hermans[17] and Hosemann[18] we know that the domain structure of polymers is not only given by their composition, but also by their disorder. Very frequently we observe domain clusters with short-range order only. Thus performing the simple correlation function analysis, the statistical face of domain structure remains unconsidered, because the domain size distributions are difficult to find in the correlation function.

The chord distribution, on the other hand, is somewhat more appropriate. In 1948 Porod[19] has used the fact that the chord distribution of a particle is the second derivative of its autocorrelation

function. For a general two-phase system the chord distribution has been introduced and studied by Méring and Tchoubar.[20,21] For a lamellar system it is reasonable to study the one-dimensional correlation function. In analogy to this definition even a *one-dimensional chord distribution* can be defined and studied for a multiphase system, which is built from stacked layers. As Ruland[9] has shown, this interface distribution function (IDF) can be expressed in a simple series of the layer thickness distributions, which characterize the lamellar domains. Thus the IDF is an appropriate basis for the study of composition and disorder of a lamellar two-phase system, as far as short and medium range disorder is concerned.

By a Fourier–Bessel transformation of $\tilde{G}_{id}(s)$

$$g_1(x) = \pi \int_0^\infty \tilde{G}_{id}(s)\left[4J_0(2\pi xs) - 2\left(2\pi xs + \frac{1}{2\pi xs} \right) J_1(2\pi xs) \right] ds \quad (3)$$

the interface distribution function (IDF) $g_1(x)$ is computed.

A quantitative IDF analysis using a model of stacked layers is meaningful, if both the polyethylene and the elastomer component exhibit lamellar two-phase systems. Because of the known fact that S1429 and S3530 show cylindrical polystyrene domains in a polybutadiene matrix, such an analysis leads to a fit with an improper model concerning the SBS component, but it is not our intention to analyze the domain structure inside the SBS grains. We use the two-component model only in order to separate the scattering of the SBS grains from the scattering of the PE grains and discuss only the structural parameters of the PE grains. Because of the imperfect superstructure inside the SBS grains we expect that the shape of the scattering curve of those grains can sufficiently be modeled by a one-dimensional model. The PS fraction of S1846 is so high that the structure of this material is supposed to consist of alternating PS and PB layers.

Hashimoto[22] and co-workers have proposed a theoretical model for the scattering of a lattice from long cylinders packed with hexagonal symmetry and distorted by paracrystalline disorder. They have successfully applied this model to the SAXS of blends from two miscible block copolymers which exhibit a latticelike domain arrangement with little distortions. In our case the distortions are significantly higher and thus a much simpler model should suffice to extract the scattering of the semicrystalline polyethylene from the compound scattering curve.

In the case of a lamellar two-phase system the IDF is composed from a series of distance distributions, $h_i(x)$. The centers of gravity of the first two distributions, $\bar{d}_1$ and $\bar{d}_2$, represent the average thicknesses of the layers of *Phase 1* and *Phase 2,* respectively. Assuming one-dimensional stacking statistics as defined by J. J. Hermans,[17] the IDF can be constructed from only $h_1(x)$ and $h_2(x)$. According to Brämer[23] the chosen statistical model overcomes the shortcoming of the paracrystalline stack, in which adjacent "crystalline" domains must penetrate each other, if considerable disorder is assumed. The model fits the measured data. Parameters of the PE component in the model are the average thicknesses of the amorphous and the crystalline layers, $\bar{d}_a = \bar{\mathrm{d}}_1$ and $\bar{d}_c = \bar{\mathrm{d}}_2$, the relative widths $\sigma_a/\bar{d}_a$ and $\sigma_c/\bar{d}_c$ of the distance distributions (which are assumed to be Gaussian), a parameter σ_H which serves to skew the Gaussians and finally the integral of the IDF, W. The observed relative width of a thickness distribution $h_i(x)$ is a function of both $\sigma_i/\bar{d}_i$ and σ_H, and can be computed from the model parameters resulting from the fit[10]

$$((\sigma_i/\bar{d}_i)^2_{\mathrm{obs}} + 1) = ((\sigma_i/\bar{d}_i)^2 + 1)(\sigma_H^2 + 1). \quad (4)$$

A second model component with a second set of parameters can be used to represent the SBS elastomer in a composite model function. Both the one- and the two-component model are fitted to the IDFs of the samples utilizing the simplex algorithm[24] for nonlinear regression, as has been described in a previous article.[10]

RESULTS AND DISCUSSION

The intermixing of the elastomer and the HDPE in the blend has been studied by TEM. Figure 1 shows transmission electron micrographs obtained after staining. The dark phase represents the elastomer as a whole and the light phase can be identified by the HDPE grains. One observes typical grain sizes between 1 and 6 μm. Thus to a first approximation, block copolymer and homopolymer appear not to be mixed on a molecular scale.

Figure 2 shows the variation of mechanical

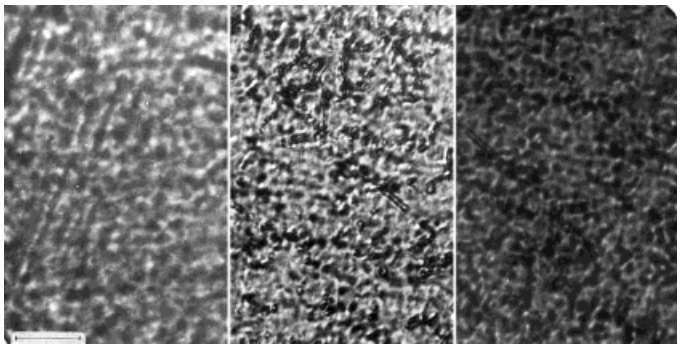

Figure 1. TEM micrographs of three blends of HDPE and S1429. Staining has been carried out by O_sO_4. The dark phase contains the elastomer.

properties of the samples in a Petrich diagram. Here tensile stress at break, σ_b, is plotted versus impact resistance, a_n. Every symbol represents one of the studied samples. Connecting lines indicate samples which are blended with the same block copolymer. So three different series start from the pure HDPE sample in the upper left corner of the diagram. Three samples, indicated by the digits (1), (2), and (3), are special. With the exception of these special samples, the SBS weight fraction varies by 5% between two marks from the diagram, which are directly connected by a line. The special sample (1) contains 2.5 wt % of S1429, sample (2) contains 12.5 wt % of S3530 and sample (3) is a ternary blend containing 2.5% of S1429 and 12.5% of S3530.

All blends exhibit lower tensile strength than pure HDPE, but those samples blended with SBS grades containing 30% PS show a considerable increase of shock resistance, as long as the SBS content does not exceed 20 wt %. The blend containing 15 wt % of S1429 manifests the best mechanical properties. Here, compared to the pure HDPE, tensile strength has decreased by 16% only, while the shock resistance has increased by a factor of 9. Blends containing the high molecular weight grade S3530 perform not as good. The sample with 12.5 wt % of SBS has the best mechanical properties of the series, but even higher is the shock resistance, if a ternary blend (rightmost circle) with a low quantity of low molecular weight SBS is prepared.

The densities of all the samples have been measured in a density gradient tube. The density of the SBS grades is very close to the density of the pure HDPE and the densities from different lots with the same blend composition vary by ± 0.003 g/cm^3. We observe a faint decrease of density with increasing SBS content, which is in good agreement with the assumption of a constant PE crystallinity.

Figure 3 shows $s\tilde{I}(s)/V$, the slit-smeared SAXS curves of the blends as measured with the Kratky camera after multiplication of the intensity by s. Thus the areas under the curves are proportional to the scattering power Q of the samples. In the S1429-series one observes that there is no trend in the curves for $s < 0.03$/nm. By preparing several lots of every blend and measuring the SAXS it has been found that the effect is due to some irreproducibility in the processing of the blend. But after the data have been transformed into the interference function (Fig. 4), no differences can be observed among the different preparations. This finding shows that we can reproduce the structure controlling medium range correlations among the domains (e.g., among a crystalline layer and its neighbors), but there is some irreproducibility concerning longer range correlations, which do not show up in the interference function and in the IDF.

A hint to the nature of the observed irreproducibility can be obtained by comparing with the scattering curve of pure S1429. Because the uncontrolled bulging of the curve occurs at a scattering angle, which corresponds to the long period of the pure block copolymer, it is most likely that we are not able to control the perfection and the arrangement of polystyrene domains in the polybutadiene matrix.

The strong peak in each of the scattering curves is the long period reflection, corresponding to an average distance between two neighboring domains. Its width is, to a first approximation, a measure of irregular arrangement. In all the series, with increasing SBS content this reflection first becomes higher, then it broadens and decreases, and finally a new strong reflection grows.

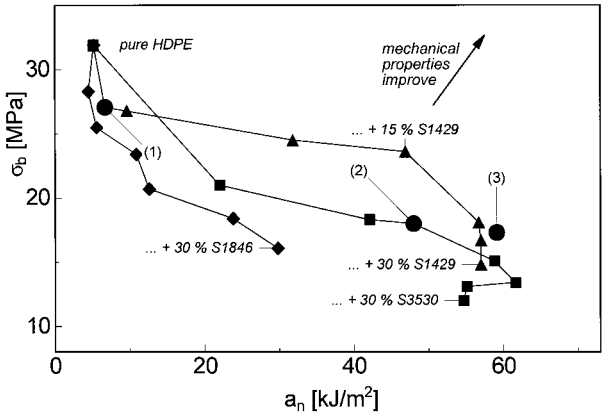

(a)

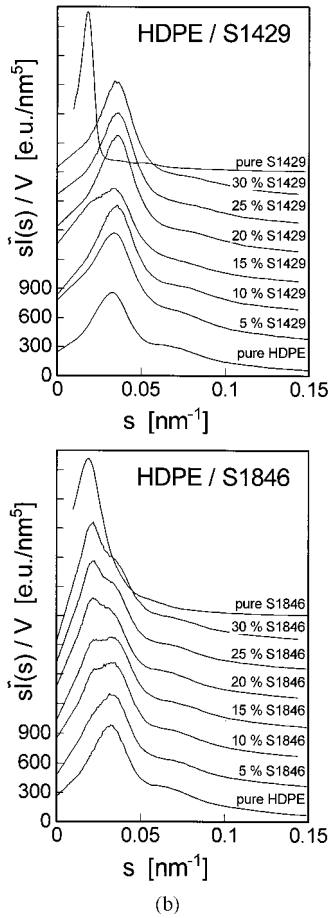

(b)

Figure 2. Variation of mechanical properties by blending of HDPE with different SBS grades. In a Petrich diagram tensile stress at break, σ_b, is plotted versus impact resistance, a_n. ▲: Blends containing S1429; ◆: Blends containing S1846; ■: Blends containing S3530. The SBS weight fraction varies by 5% between two connected marks—except the three circular marks, which designate special samples labeled by digits: (1) contains 2.5 wt % of S1429, Sample (2) contains 12.5 wt % of S3530, and Sample (3) is a ternary blend containing 2.5% of S1429 and 12.5% of S3530.

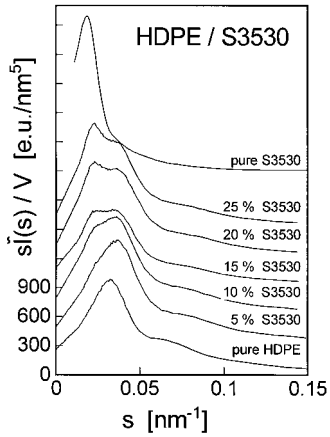

Figure 3. Absolute SAXS intensities $\tilde{I}(s)/V$ measured with a Kratky camera after multiplication by s, the magnitude of the scattering vector. The area under the curve is proportional to the scattering power Q of the samples. Each diagram shows one of the three series of blends with a different SBS.

The position of the peak observed for low SBS content is the same for each blend (and corresponds to the long spacing of PE).

Figure 4 shows the interference functions for one of the series after removal of the extra peak in the Porod region and smoothing the data using cubic splines and a natural smoothing parameter.[25] Raw data before smoothing and the interpretation of the extinguished peak in terms of density undulations are presented elsewhere.[7]

Using eq. (3), the curves are transformed into the IDF's, which are shown in Figure 5. The variable x in the diagram is the direction perpendicular to the stacks of alternating layers (amorphous/crystalline or PS/PB, respectively). The positive peaks correspond to the domain thickness distributions, the negative peak originates from the distribution of the long spacings. The fact that all the curves do not vanish in the vicinity of zero shows that the domain interfaces are rough. The effect of such a roughness on the scattering data has been discussed by others.[12,13] If the phase boundary between adjacent domains is rough, there are many chords of very short length (or layers of almost zero thickness). In the IDF this leads to a considerable contribution in the vicinity of zero, an effect which virtually shifts the center

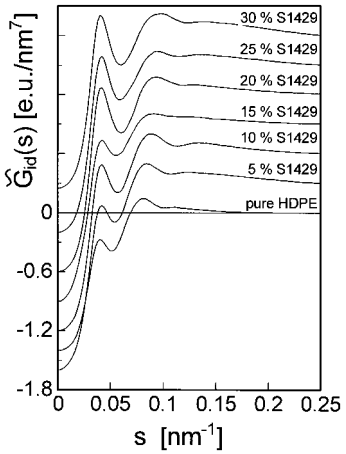

Figure 4. HDPE/S1429 blends. Interference functions $\tilde{G}_{id}(s)$ obtained from the measured data (cf. Fig. 3) by application of eq. (1). In the tail of the curves with low SBS content an extra peak has been extinguished as described in the Data Analysis Section.

of the first thickness distribution towards a lower value.

The IDF of the pure PE is the only curve which can be fitted by a model with only one component. Here we obtain an average amorphous layer thickness, $\bar{d}_a$ = 4 nm and a mean crystalline thickness, $\bar{d}_c$ = 18.7 nm. We compute a long spacing $\bar{L}$ = 22.7 nm and a volume crystallinity $\Phi_c = \bar{d}_c/\bar{L}$ = 0.82. Taking into account the considerable roughness of the domain surfaces, the agreement with the value computed from density (cf. section "Material") is good.

As an example, Figure 6 demonstrates the quality of the fits and Table II shows the fit parameters determined for one complete series (HDPE blended with S3520). With respect to the PE component, $\bar{d}_1$ and $\bar{d}_2$ represent the average thicknesses of the amorphous lamellae and of the crystalline lamellae, respectively. For SBS components from a blend, $\bar{d}_1$ is related to the PS domain diameter, while $\bar{d}_2$ is related to the distance between them. The ratio $\bar{d}_1/(\bar{d}_1 + \bar{d}_2)$ and magnitude of these parameters agree with the PS content of the block copolymer S3530 and with the expected microstructure.

Not the model-intrinsic width parameters, but only the observable relative distribution widths $(\sigma_i/\bar{d}_i)_{obs}$ (according to eq. (4)) are of physical meaning and shall be discussed. The computed values are presented in Table III. Scanning all the resulting parameter values for the three studied series, one observes little spectacular results. No significant change is observed in the structure inside the SBS grains. Inside the PE grains the average thicknesses of the crystalline and the amorphous PE layers remain constant (the initial decrease is most probably only an artifact caused by the switching from a one-component to a two-component model function). No change is found for the observed widths of the distribution of crystalline layer thicknesses, as well.

On the other hand, a significant variation is found for the width of the distribution of the amor-

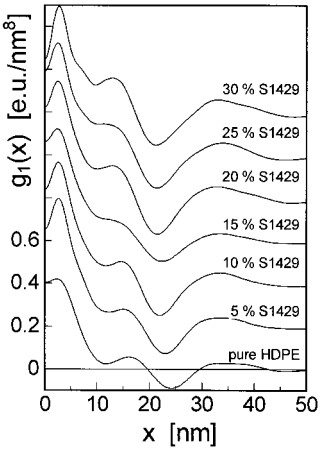

Figure 5. HDPE/S1429 blends. Interface distribution functions (IDF) $\tilde{G}_{id}(s)$ obtained by Fourier–Bessel transformation of the interference functions (cf. Fig. 4). The positive peaks result from the domain thickness distributions. The negative peak corresponds to the distribution of long spacings.

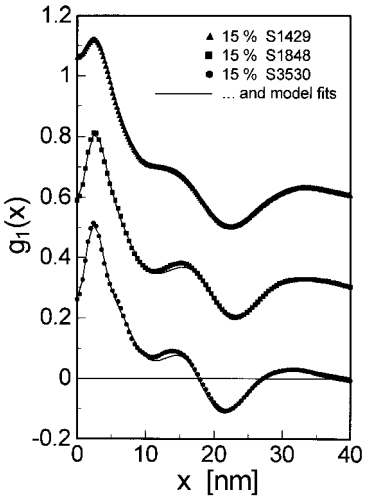

Figure 6. Fits of the IDFs from blends containing 15 wt % SBS with a function modeling two different kinds of lamellar stacks.

Table II. Blends of HDPE and the Block Copolymer S3530. Parameter Values Determined by Fitting the Scattering Data (IDF) With a Two-Component Model of Stacked Layers. *W:* Strength of the Component (in Units of the Porod's Asymptote A_{P_1}). $\bar{d}_1$, $\bar{d}_2$: Average Layer Thicknesses. σ_H: Skewing Parameter of the Layer Thickness Distributions. $\sigma_1/\bar{d}_1$, $\sigma_2/\bar{d}_2$: Model-Intrinsic Relative Width of the Layer Thickness Distributions. The Indicated Intervals of Confidence Are Estimated from the Quality of the Fit.[26]

SBS Fraction	Component	W [e.u./nm^7]	$\bar{d}_1$ [nm]	$\bar{d}_2$ [nm]	σ_H	$\frac{\sigma_1}{\bar{d}_1}$	$\frac{\sigma_2}{\bar{d}_2}$
0	SBS	–	–	–	–	–	–
	PE	2.8 ± 0.1	3.9 ± 0.1	18.7 ± 0.4	0.25 ± 0.01	0.55 ± 0.01	0
5	SBS	1.2 ± 0.1	6.4 ± 0.2	17.0 ± 0.6	0.20 ± 0.04	0.22 ± 0.05	0.21 ± 0.04
	PE	2.2 ± 0.1	2.6 ± 0.1	17.9 ± 0.2	0.13 ± 0.01	0.49 ± 0.01	0.13 ± 0.01
10	SBS	1.1 ± 0.2	6.7 ± 0.3	17.9 ± 0.7	0.20 ± 0.05	0.22 ± 0.06	0.24 ± 0.04
	PE	2.0 ± 0.1	2.7 ± 0.2	17.8 ± 0.3	0.15 ± 0.02	0.53 ± 0.01	0.11 ± 0.02
15	SBS	1.0 ± 0.2	6.6 ± 0.4	17.8 ± 1.2	0.21 ± 0.07	0.23 ± 0.09	0.22 ± 0.07
	PE	1.9 ± 0.2	2.5 ± 0.2	17.9 ± 0.4	0.15 ± 0.03	0.61 ± 0.01	0.10 ± 0.03
20	SBS	1.0 ± 0.2	6.7 ± 0.4	17.6 ± 1.4	0.21 ± 0.09	0.22 ± 0.1	0.22 ± 0.09
	PE	1.8 ± 0.2	2.6 ± 0.2	16.9 ± 0.5	0.15 ± 0.03	0.57 ± 0.01	0.09 ± 0.04
25	SBS	1.0 ± 0.4	8.3 ± 1.1	21 ± 11	0.31 ± 0.54	0.27 ± 0.38	0.32 ± 0.27
	PE	1.8 ± 0.4	2.9 ± 0.2	17.9 ± 0.7	0.17 ± 0.04	0.57 ± 0.02	0.07 ± 0.05

phous layers inside the polyethylene grains as a function of SBS content (Fig. 7). Addition of the lower molecular weight SBS grade S1429 widens the distribution of the amorphous PE layers (triangles), while there is some initial decrease of these widths when blended with the higher molecular weight block copolymers. This initial decrease is not considered as an artifact, since we observe the narrowing of the long period reflection in the measured data (Fig. 3), too.

For all the series there is a local maximum at 15 wt % of SBS content. Thus by means of the IDF analysis the observed broadening of the SAXS peak (cf. Fig. 3) at this characteristic blend composition can be attributed to a widely fluctuating thickness of amorphous PE-layers about their mean value. Such an extra fluctuation generates a fluctuation of the long spacing, as well. Now one might argue that the chosen model would compensate an increased roughness of the domain interfaces just by attributing an enlarged width to the domain thickness distribution, which is placed closest to $x = 0$ (and this is the distribution of the amorphous polyethylene layers discussed here). But apart from the fact that in this case one would expect the parameter $\bar{d}_1$ shifted to smaller values of x simultaneously, one would

Table III. Blends of HDPE and the Block Copolymer S3530. Observable Relative Domain Thickness Distribution Widths $(\sigma_1/\bar{d}_1)_{obs}$ and $(\sigma_2/\bar{d}_2)_{obs}$ Computed from the Values in Table II using eq. (4)

SBS Fraction	Component	$\left(\frac{\sigma_1}{\bar{d}_1}\right)_{obs}$	$\left(\frac{\sigma_2}{\bar{d}_2}\right)_{obs}$
0	SBS	–	–
	PE	0.62	0.25
5	SBS	0.30	0.29
	PE	0.51	0.19
10	SBS	0.30	0.32
	PE	0.56	0.19
15	SBS	0.32	0.31
	PE	0.64	0.18
20	SBS	0.31	0.31
	PE	0.60	0.18
25	SBS	0.42	0.46
	PE	0.60	0.18

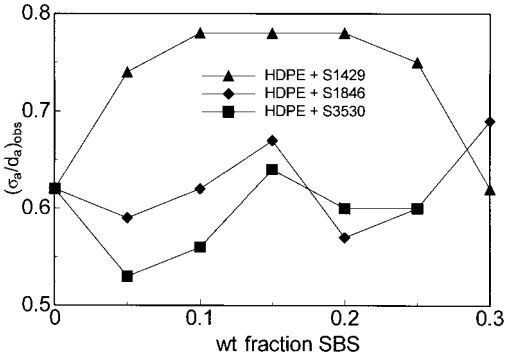

Figure 7. Observed relative width of the distribution of amorphous layer thicknesses inside the polyethylene grains of the heterogeneous blend as a function of SBS content and composition.

not be able to observe a broadening of the long period reflection (Fig. 3).

In summary, the shape of the SAXS curve of HDPE/SBS blends as a function of blend composition reveals some component interaction close to 15 wt % SBS content by a considerable broadening of the long period reflection. An IDF analysis shows that this broadening is mainly caused by an increase of thickness fluctuations of only the amorphous layers in the HDPE stacks about a constant average thickness. The strength of this interaction is predominantly a function of the molecular weight of the SBS component (cf. Fig. 7). Low molecular weight SBS has the strongest; high molecular weight the weakest, effect on the amorphous zones inside the PE grains.

The IDF analysis shows that the mechanical mixing of the two polymers involves not only a mixing on macroscopic scale. The miscibility of short-chain SBS with the amorphous PE from the stacks can be detected by its effect on the disorder of the stacks. In the case of the block copolymer S1429, the PE domains appear to be almost saturated with only 5 wt % S1429 in the material. In order to test this notion, we have prepared three additional samples and measured the mechanical properties. In Figure 2 these samples are marked by circles. The rightmost circle describes a ternary blend, which contains 15% of SBS, but instead of taking 15% of S3530, 2.5% of the SBS has been exchanged by S1429. Thus, due to the increased miscible fraction of SBS, the compatibility between the components should increase. In the diagram we observe the effect on the mechanical properties. The impact resistance remains constant, and the tensile stress at break increases, since the coupling between SBS and PE has been enhanced. The leftmost of the circles shows that this enhancement of the tensile strength is only a relative one. Compared to the pure HDPE the material loses strength, since inner surface is generated.

Thus there is no synergistic effect concerning material properties with respect to pure polyethylene. But with respect to the binary blend containing S3530, the ternary blend chosen shows an improvement of both reported mechanical parameters. This result lets the search for a synergistic effect with blends made from postconsumer plastics appear promising.

We have presented SAXS curves from HDPE/SBS blends, which exhibit a peculiar feature as a function of blend composition. Up to an SBS content of 15 wt % the fluctuation of the thicknesses of the amorphous layers in the HDPE grains about their average thickness increases and faint density undulations can be detected in the SAXS curves. Beyond an SBS content of 15 wt % the density undulations become negligible and the thickness of the amorphous PE layers, again, becomes more precise.

CONCLUSION

A quantitative analysis of the SAXS curves from HDPE/SBS blends as a function of blend composition can take into account arrangement and disorder of the two-phase structure inside the HDPE and the SBS grains dispersed in the heterogeneous blend. Comparison of the results of this method with the mechanical properties of the material yields deeper insight into the structural features, which cause improvement of material performance. One can thus determine, where in the local structure of the HDPE the compatibilizer SBS increases the disorder.

SAXS analysis shows that the roughness of the domain interfaces in these samples is considerable. If one could reduce this roughness of the interface, one would probably be able to study structural variations in more detail. A practical step towards the reduction of domain surface roughness could perhaps be undertaken by annealing the samples.

The authors gratefully acknowledge the support of this study by the Romanian Ministry for Research and Technology and the German Ministry for Education and Research in the frame of the German–Romanian Cooperation in Science and Technology (Project X055.4).

REFERENCES AND NOTES

1. M. Xanthos, A. Patel, S. Dey, S. S. Dagli, C. Jacob, T. J. Nosker, and R. W. Renfree, *Adv. Polym. Technol.,* **13,** 239 (1994).
2. B. Brahimi, A. Ait-Kadi, A. Ajji, and R. Fayt, *J. Polym. Sci. Part B: Polym. Phys.,* **29,** 945 (1991).
3. D. S. Chiu, Z. Zhang, and G. C. Siu, *J. Reinf. Plast. Compos.,* **15,** 74 (1996).
4. Z. Wang, *J. Appl. Polym. Sci.,* **60,** 2239 (1996).
5. P. Hedenberg and P. Gatenholm, *J. Appl. Polym. Sci.,* **56,** 641 (1995).
6. E. Ceausescu, P. Ghioca, H. Paven, G. Banica, E. Buzdugan, I. Cerchez, R. Stancu, A. Ion, and D. Mardare, *Rev. Roum. Chim.,* **34,** 711 (1989).

7. N. Stribeck, P. Ghioca, and E. Buzdugan, *J. Appl. Cryst.,* **30,** 708 (1997).
8. N. Stribeck, *Macromolecules,* **29,** 7217 (1996).
9. W. Ruland, *Colloid Polym. Sci.,* **255,** 417 (1977).
10. N. Stribeck, *Colloid Polym. Sci.,* **271,** 1007 (1993).
11. W. Ruland, *J. Appl. Cryst.,* **4,** 70 (1971).
12. W. Ruland, *Macromolecules,* **20,** 87 (1987).
13. A. N. Semenov, *Macromolecules,* **27,** 2732 (1994).
14. P. Debye and A. M. Bueche, *J. Appl. Physics,* **20,** 518 (1949); P. Debye, H. R. Anderson, Jr., and H. Brumberger, ibid. **28,** 679 (1957).
15. G. Porod, *Kolloid-Z. u. Z. Polymere,* **124,** 83 (1951); **125,** 51 (1951).
16. C. G. Vonk and G. Kortleve, *Colloid Polym. Sci.,* **220,** 19 (1967).
17. J. J. Hermans, *Rec. Trav. Chim. Pays-Bas,* **63,** 211 (1944).
18. R. Hosemann, *Z. Phys.,* **127,** 16 (1949).
19. G. Porod, *Acta Phys. Austriaca,* **2,** 286 (1948).
20. J. Méring and D. Tchoubar, *J. Appl. Cryst.,* **1,** 153 (1968).
21. D. Tchoubar and J. Méring, *J. Appl. Cryst.,* **2,** 128 (1969).
22. T. Hashimoto, T. Kawamura, M. Harada, and H. Tanaka, *Macromolecules,* **27,** 3063 (1994).
23. R. Brämer, *Kolloid-Z. u. Z. Polymere,* **252,** 504 (1974).
24. M. S. Caceci and W. P. Cacheris, *Byte,* **May,** 340 (1984).
25. C. H. Reinsch, *Numer. Math.,* **16,** 451 (1971).
26. N. R. Draper and H. Smith, *Applied Regression Analysis,* John Wiley, New York, 1966, pp. 263–306.